

LYSO-based Precision Timing Detectors with SiPM Readout

A. Bornheim^a, M. H. Hassanshahi^b, M. Griffioen^a, J. Mao^a, A. Mangu^a, C. Peña^a,
M. Spiropulu^a, S. Xie^{*,a}, Z. Zhang^a

^a*California Institute of Technology, Pasadena, CA, USA*

^b*Institute for Research in Fundamental Science, Tehran, Iran*

Abstract

Particle detectors based on scintillation light are particularly well suited for precision timing applications with resolutions of a few 10 ps. The large primary signal and the fast initial rise of the scintillation light result in very favorable signal-to-noise conditions with fast signals. In this paper we describe timing studies using a LYSO-based sampling calorimeter with wavelength-shifting capillary light extraction and silicon photo multipliers as sensors. We study the contributions of various steps of the signal generation to the total time resolution, and demonstrate its feasibility as a radiation-hard technology for calorimeters at high intensity hadron colliders.

Key words: LYSO, Silicon Photomultiplier, Precision Timing, picosecond, scintillation, calorimeter

1. Introduction

Scintillating materials are widely used in detectors of ionizing radiation. They are very common as primary sensors in calorimetric applications, either serving simultaneously as an absorber material, such as solid crystals, or in combination with passive absorbers in a layered arrangement, referred to as sampling calorimeters. Scintillators are also used to detect charged particles where they achieve a very high efficiency with a layer of thickness of about a few millimeters. LYSO has been proposed as a scintillating crystal for future calorimeters due to its large scintillation light yield [1, 2]. To convert the primary scintillation light signal into an electrical signal a photodetector is coupled to the scintillator volume, either directly or via a light guiding structure. Silicon Photo Multipliers (SiPM) are a common choice as a photodetector in contemporary applications. In this paper we present studies on SiPMs and a LYSO-based sampling calorimeter with SiPM readout with a focus on precise timing measurements.

Precise time of arrival measurements have recently drawn much attention in the context of detector R&D for the high luminosity upgrade of the Large Hadron Collider (HL-LHC) as well as for future high energy hadron colliders. These hadron colliders must provide large instantaneous luminosity well above $10^{35} \text{ cm}^{-2}\text{s}^{-1}$. With current

*Corresponding author

Email address: sixie@hep.caltech.edu (S. Xie)

Preprint submitted to Nucl. Instrum. Meth. A

August 22, 2017

accelerator and particle detector capabilities, such a high instantaneous luminosity will result in very large amounts of simultaneous particle collisions (pileup) exceeding several hundreds per bunch crossing. Therefore, the crucial ability to identify the origin of the particles produced at the different interaction points will be severely degraded. Precision timing detectors can be used to recover the ability to discriminate between particles produced by different inelastic collisions [3]. For particle beams with bunch profiles similar to that of the LHC, a detector that can measure the time of arrival of all final state particles with a precision of 20 – 30 ps can effectively reduce the impact of pileup by a factor of 5 to 10.

With a timing resolution below 10 ps for individual charged particles, the equivalent spatial resolution is sufficiently good to improve the performance of track reconstruction [4] for hadron collider experiments. A timing resolution in the picosecond range for photons is also very interesting for optical time projection chambers which are discussed for large volume detectors in neutrino experiments and neutrino-less double-beta decay [5, 6].

The paper is organized as follows. In Sec. 2 we give a brief overview of the SiPM sensors in the context of our research. In Sec. 3 we describe the experimental techniques we employ in our precision timing measurements as well as the specific setups we used for the studies presented in this paper. In Sec. 4.1 we present the results of timing measurements using SiPMs as photodetectors to read out scintillation light from LYSO crystals exposed to electrons in the GeV energy range. In Sec. 4.2 we evaluate the impact of the intrinsic timing performance of SiPM devices on the calorimeter time measurement by measuring the time resolution for SiPMs injected with light from a fast laser.

2. SiPM

Silicon Photomultipliers (SiPM) are pixelated photodetectors that are widely used in contemporary high-energy physics experiments. Their compactness and form factor make them ideal for many applications including calorimeters, charged particle detectors, and positron emission tomography detectors. The size of each SiPM device typically ranges between $1 \times 1 \text{ mm}^2$ and $6 \times 6 \text{ mm}^2$, with the size of each pixel ranging between $10 \mu\text{m}$ to $50 \mu\text{m}$. SiPMs operate at relatively high gain between 10^5 and 10^6 , and have single photon detection efficiency ranging from 10% to 50%. As each pixel operates in geiger mode, it is essentially a digital device. More than one photon impinging on a single pixel yields the same signal as a single photon impinging on that pixel. Therefore as the number of photons approaches the total number of pixels, the SiPM experiences a slow saturation as the signal response slowly becomes non-linear. Total saturation occurs if the number of photons exceed the number of pixels in the device.

SiPMs have a typical thermal dark count rate of about 1 MHz, which can be strongly decreased when operated at lower temperatures. Typical operational temperatures range from 20 to 30 degrees Celsius, but can be as low as -30 degrees Celsius. SiPMs have been tested for the impact of radiation damage up to an equivalent neutron rate of $2 \times 10^{14} \text{ cm}^{-2}$, and its performance have been shown to be robust when operated at temperatures below 5 degrees Celsius. [7, 8]. However, when operated at the same temperature, the thermal dark count rate increases significantly with large irradiation.

The SiPMs used for our studies are Hamamatsu MPPC S12571-010P and S12571-015P both of size $1 \times 1 \text{ mm}^2$, and S12572-15C and S12572-25C both of size $3 \times 3 \text{ mm}^2$.

Some relevant details of the SiPM parameters are summarized in Table 1 below.

Table 1: Summary of performance parameters for SiPMs used in our studies.

Parameter	S12571-010C	S12571-015C	S12572-15C	S12572-25C
Photosensitive area	$1 \times 1\text{mm}^2$	$1 \times 1\text{mm}^2$	$3 \times 3\text{mm}^2$	$3 \times 3\text{mm}^2$
Pixel Pitch	$10\mu\text{m}$	$15\mu\text{m}$	$15\mu\text{m}$	$25\mu\text{m}$
Number of Pixels	10000	4489	40000	14400
Dark Count Rate	0.1 MHz	0.1 MHz	1 MHz	1 MHz
Gain	1.35×10^5	2.3×10^5	2.3×10^5	5.15×10^5
Terminal Capacitance	35 pF	35 pF	320 pF	320 pF
Spectral Response Range	320-900 nm	320-900 nm	320-900 nm	320-900 nm
Peak Sensitivity Wavelength	470 nm	460 nm	460 nm	450 nm

3. Setup and Experimental Apparatus

We performed measurements of SiPM properties in the laboratory at Caltech using signals from a class 3R PiLas laser which produces light at a wavelength of 407 nm. Beam measurements were performed at the H4 beam-line of the CERN North-Area test-beam facility, which provides secondary beams of energies ranging between 20 GeV and 400 GeV. The beams are composed of a mixture of electrons and pions. The electron fraction in the beam is typically around 75%.

The data acquisition (DAQ) system uses a CAEN V1742 switched capacitor digitizer based on the DRS4 chip [9], whose electronic time resolution has been measured to be 4 ps. Data readout for the laser-based measurements are triggered by an external digital trigger signal, while at the H4 beamline readout is triggered by a signal in a photomultiplier tube coupled to a 3 cm \times 3 cm plastic scintillator located about one meter upstream from our detectors. A micro-channel plate photo-multiplier (MCP-PMT) detector is used to provide a very precise reference time-stamp in order to measure the time resolution of the SiPM signals.

3.1. Setup for Laser-based SiPM Timing Measurements

SiPMs are mounted on a printed circuit board (PCB) with a clipping capacitance circuit shown in Figure 1. They are mechanically attached to an optical breadboard enclosed within a box lined with copper foil for RF shielding. The laser is injected via a light-guide fiber mounted on an optical holder. The laser beam is immediately split by a 50/50 beam splitter and half of the light is directed onto the MCP-PMT while the other half of the light is directed onto the SiPM under test. A photograph of the setup is shown in Figure 2. The Photek-240 MCP-PMT is used as the reference time detector whose time resolution has been measured to be below 7 ps for beam particles [10]. To cover a large range of laser beam intensity, neutral density (ND) filters with ND number between 0.2 and 2.4 are placed between the beam splitter and the SiPM under test.

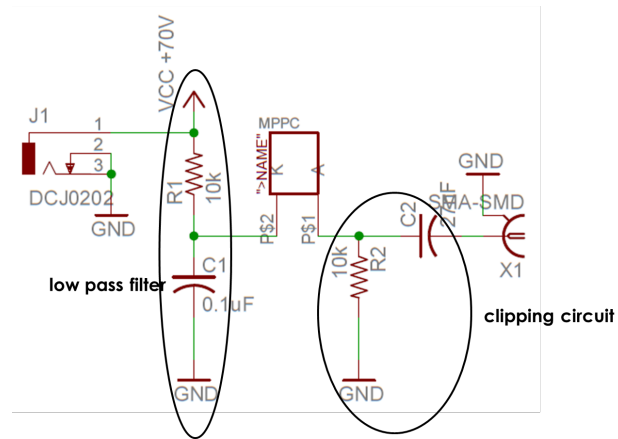


Figure 1: A schematic diagram of the circuit used to read out the SiPMs.

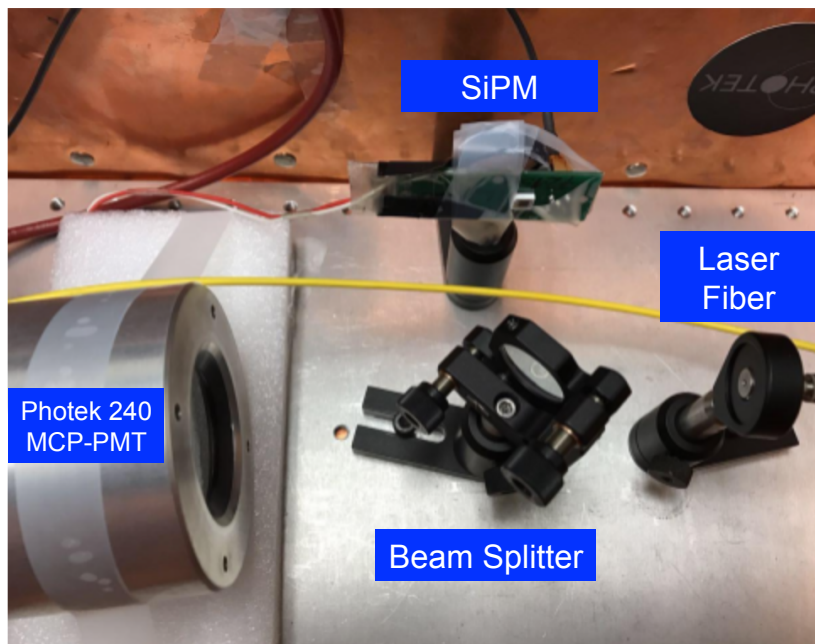


Figure 2: Photograph of the Laser-based SiPM timing measurement setup.

3.2. Setup for Timing Measurements of Scintillators with SiPM readout.

The experimental setup we use for the calorimetric timing measurements consists of a single cell of a sampling calorimeter with 29 alternating layers of LYSO crystal and tungsten absorber. This arrangement is known as a Shashlik sampling calorimeter configuration. The lateral dimensions are $14 \times 14 \text{ mm}^2$. The total depth of the cell is about 11.5 cm with the LYSO layers having a thickness of 1.5 mm. The same cell has been used to measure the timing performance in comparison to the timing performance of a single monolithic crystal of LYSO [11]. A scintillator counter of size $1 \times 1 \text{ cm}^2$, mounted close to the calorimeter cell, is used to select events impinging on the calorimeter cell and to filter out. The scintillation light from the LYSO plates is extracted with four wavelength-shifting (WLS) fibers. The fibers are coupled to four different types of Hamamatsu SiPMs with 10, 15 and 25 μm pixel size and $1 \times 1 \text{ mm}^2$ and $3 \times 3 \text{ mm}^2$ sensor size [12]. The SiPMs are all read out with a DRS digitizer through the clipping circuit shown above in Figure 1. The same clipping circuit as shown in Fig 1 is used for all four SiPMs. We do not amplify the output signal of the SiPMs, only exploiting the very large light yield of the LYSO scintillator and the intrinsic amplification of the SiPMs. A labeled photograph of the setup in the H4 beamline is shown in Figure 3. More details of the calorimetric performance of the Shashlik configuration are discussed in references [13] and [14].

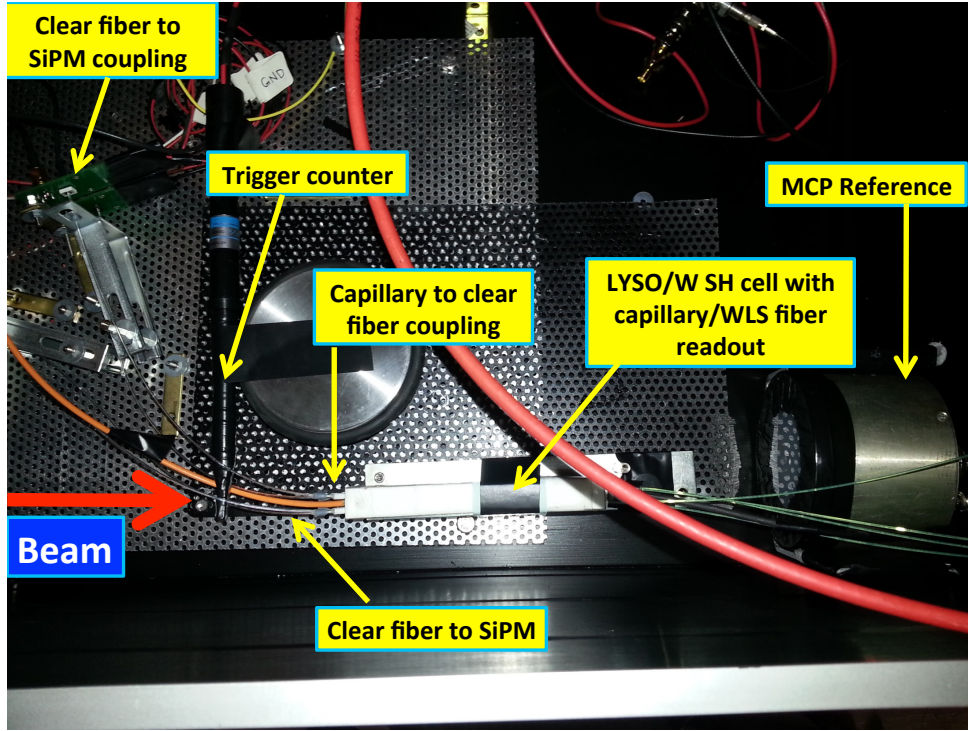


Figure 3: Photograph of the timing measurement setup in the H4 beamline.

In addition to plastic WLS fibers we also tested quartz capillaries filled with liquid wavelength shifter using DSB as a wavelength-shifting agent [15]. To optically couple the

quartz capillaries to the SiPMs we use a clear plastic fiber light guide which is connected to the end of the quartz capillary with a metal sleeve tube. The same clear fiber coupler is used for the plastic WLS fibers to maintain equivalent light collection efficiency. The ratio of the light collection efficiency between the plastic fibers and the quartz capillaries approximately scales with the ratio of the diameter of the plastic fiber and the liquid core of the quartz capillary. This ratio is about 3 for the fibers and capillaries we used.

As a timing reference we use a Photek 240 MCP-PMT. It is placed behind the calorimeter cell and detects secondary shower particles escaping from the Shashlik calorimeter cell as we did in our previous studies [11]. The time resolution is extracted by measuring the time difference between the reference counter and the calorimeter cell over an ensemble of shower events. The time stamp for the reference counter and calorimeter cell is extracted from a Gaussian fit to the peak and a linear fit to the rising edge, respectively, as described below in Section 3.3.

We measure the timing performance of the calorimeter cell with high energy electrons in a range between 20 GeV and 200 GeV in the CERN North Area test-beam. The impact point of the electrons onto the calorimeter cell is measured with a fiber hodoscope with a precision of better than 1 mm. As timing measurements are affected by shower containment, we restrict the time measurements to events where shower containment is large. This is achieved by using events where the beam particle impacts in the center of the calorimeter cell within a restricted area between $2 \times 2 \text{ mm}^2$ and $6 \times 8 \text{ mm}^2$ depending on the exact setup.

3.3. Timestamp Reconstruction

The time-stamp for all signals is reconstructed by fitting the pulse waveform with an appropriate functional form. Signal pulses from the MCP-PMTs as well as direct laser light signals on the SiPMs exhibit a very fast rise and decay. Therefore, we fit a Gaussian function to a 1.4 ns window around the peak of the pulse and extract the time-stamp as the mean parameter of the Gaussian function. Scintillation signal pulses read out by the SiPM sensors have a much longer decay time. For these signals, we fit a linear function to time sample points between 10% and 60% of the pulse maximum and the time-stamp is assigned as the time at which the fitted linear function rises to 20% of the pulse maximum. More details of the time-stamp reconstruction can be found in reference [11].

4. Timing Measurements

A previous study on precision timing with LYSO-based calorimeters [11] using MCP-PMT as the primary photodetectors achieved time resolutions at the level of about 100 ps. In this paper, we present new studies of the timing performance of LYSO-based calorimeters using SiPMs. While SiPMs feature a rise time around 1 ns, slower than the rise time of MCPs, they allow a very good timing performance for large, coherent signals. In subsection 4.1 we describe measurements of the timing performance for a LYSO-based sampling calorimeter read out by wavelength-shifting light fibers connected to SiPMs. In subsection 4.2 we discuss the impact of the intrinsic timing performance of SiPMs on the calorimeter timing measurement studied using light signals injected by a picosecond laser.

4.1. Timing Performance Results from Calorimeter with SiPM Readout

Four different SiPMs are used to read out the four light fibers. As the SiPMs and fibers each have different gain and light collection efficiency, the signal amplitude varies for the four different channels. In Figure 4 we show the time resolution of the four individual fibers as a function of their respective signal amplitudes for both the DSB-doped fibers and the DSB-filled quartz capillaries. We observe that the time resolution improves as the amplitude of the pulses increases. The best time resolution per fiber is around 60 ps for all of the channels, but the amplitude at which this performance is achieved varies. Another important observation is that the time resolution measured from the WLS fibers fall on the same curve as the time resolution measured from the quartz capillaries. We conclude that the method of light extraction impacts the time resolution only through its effect on the signal amplitude, and no additional time jitter is introduced.

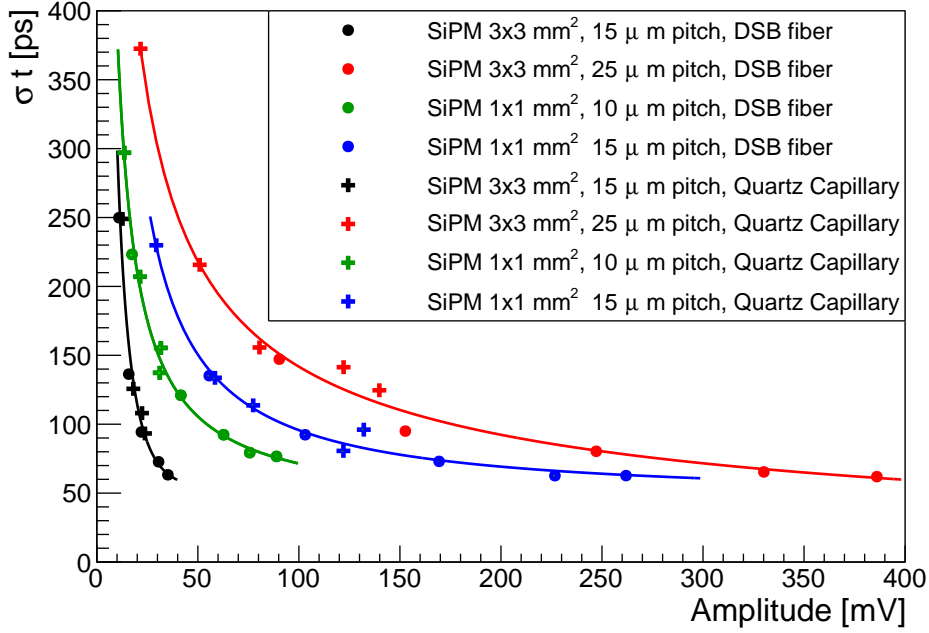


Figure 4: The measured time resolution is shown as a function of the signal amplitude for each individual read-out fiber and SiPM. The data for each SiPM consists of two sets, one with the DSB-doped WLS plastic fiber shown as dots and one with the capillaries filled with a liquid DSB-based WLS shown as squares.

As the time measurement precision depends on the rise time of the pulse we also measure the time resolution as a function of the rise time for signals observed in the calorimeter cell shown in Figure 5. The rise time of these signals are driven by the time constants of the wavelength shifter as demonstrated in reference [11]. For the data presented here, using SiPMs as photodetectors, we observe that the rise time ranges between 1.4 ns and 6 ns and that the time resolution improves roughly proportional to

the rise time of the signals. In our previous studies of the same calorimeter cell using MCPs as photodetectors [11], the rise time was measured to be around 3.0 ns. The intrinsic rise time for light signals detected by these SiPMs was measured to be 0.65 ns using a fast laser described in Sec 4.2 below. Additionally, we find that the rise time decreases with increasing amplitude, which was not observed in our previous studies using MCPs as photodetectors. Studies are ongoing to better understand this effect.

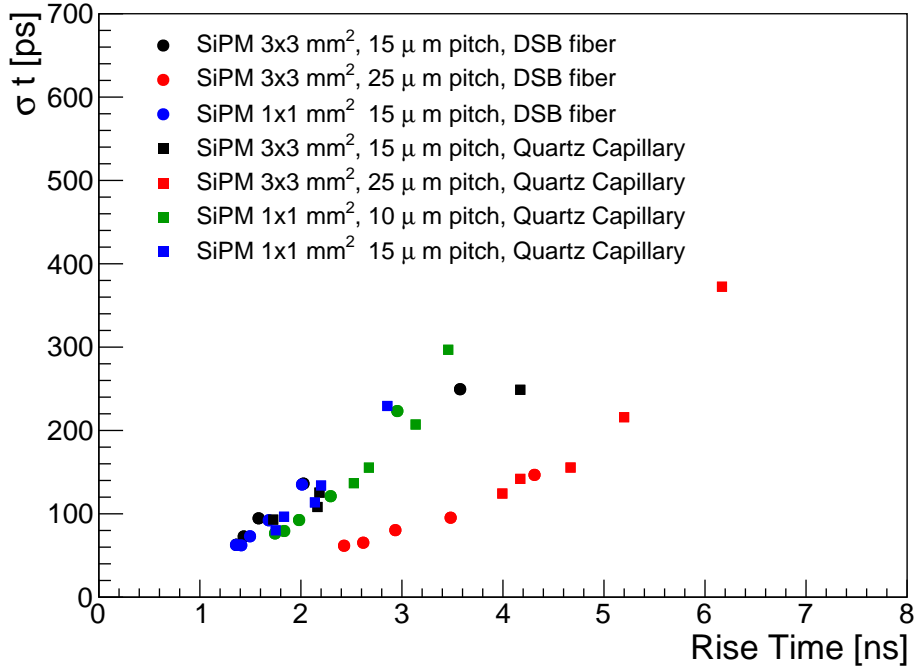


Figure 5: Time resolution is measured as a function of the rise time for the four different SiPMs. The data recorded with the DSB WLS fibers and the quartz capillaries are distinguished as dots and squares, respectively.

We show the time resolution measured as a function of the beam energy for signals read out by DSB-doped WLS fibers and quartz capillaries in Figure 6. Finally, by combining the measured timestamp from all four SiPM channels, we can significantly improve the time resolution. The combined time resolution measurements for the DSB WLS fibers and the quartz capillaries are shown in Fig 7 and demonstrate that we can achieve time resolution of 42 ps for high energy electromagnetic showers. The timing performance we achieve with the SiPM readout is slightly better than the performance achieved with an MCP-PMT as in our previous publication [11].

We should add that for the double sided MCP readout in our previous paper we achieved 90, 70, 60 ps at 50, 100 150 GeV respectively.

The light extraction efficiency of capillaries with liquid WLS remains sufficiently high for dose rates of 100 Mrad and beyond and for fluences of 10^{14} protons/cm² and beyond [14]. This result demonstrates the feasibility of achieving good time resolution

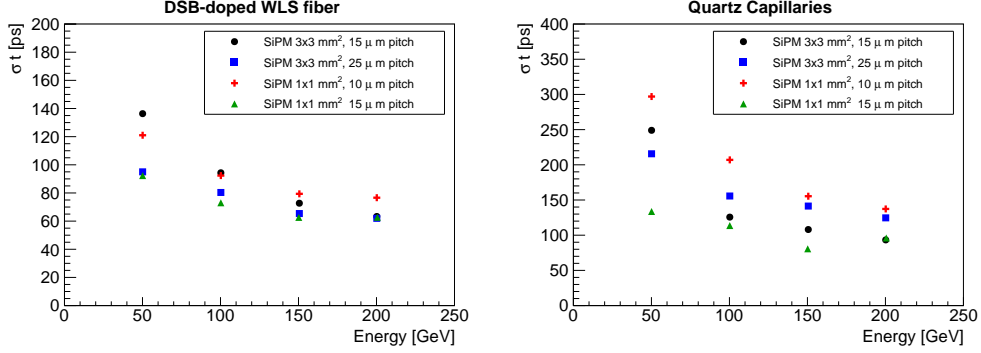


Figure 6: Time resolution measured in the sampling calorimeter cell using the signal of each of the SiPMs individually as a function of the beam energy. The data taken using DSB-doped WLS fibers are shown on the left and the data taken using DSB-filled quartz capillaries are shown on the right

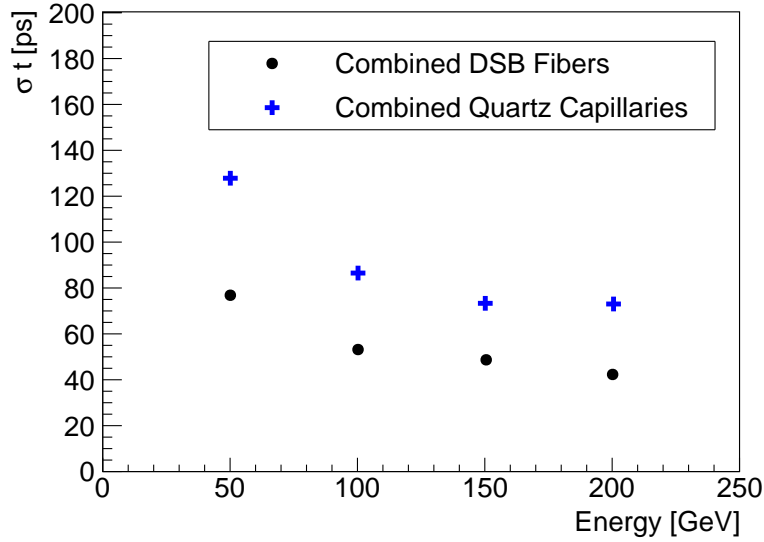


Figure 7: Time resolution measured in the sampling calorimeter cell combining signals from all four SiPMs is shown as a function of the beam energy. The data recorded with the DSB-doped WLS fibers and the DSB-filled quartz capillaries are distinguished as dots and squares.

199 using a sampling calorimeter based on LYSO which can survive in dense hadronic collision
 200 environments. The timing performance could be further improved by increasing the
 201 signal size, for example by using larger diameter capillaries or increasing the calorimeter
 202 sampling fraction.

203 4.2. Timing Performance Results for Laser Pulses

204 To evaluate the impact of the intrinsic timing performance of the SiPMs on the
 205 time resolution measured for the sampling calorimeter signals, we performed laser-based

206 measurements for two types of SiPMs: a Hamamatsu S12571-015P Multi-Pixel Photon
 207 Counter (MPPC) with an area of $1 \times 1 \text{ mm}^2$ and pixel pitch size of $15 \text{ }\mu\text{m}$, and a
 208 Hamamatsu S12572-25C MPPC with an area of $3 \times 3 \text{ mm}^2$ and pixel pitch size of $25 \text{ }\mu\text{m}$.
 209 Examples of the digitized waveforms for signals from both SiPMs are shown in Figure 8.

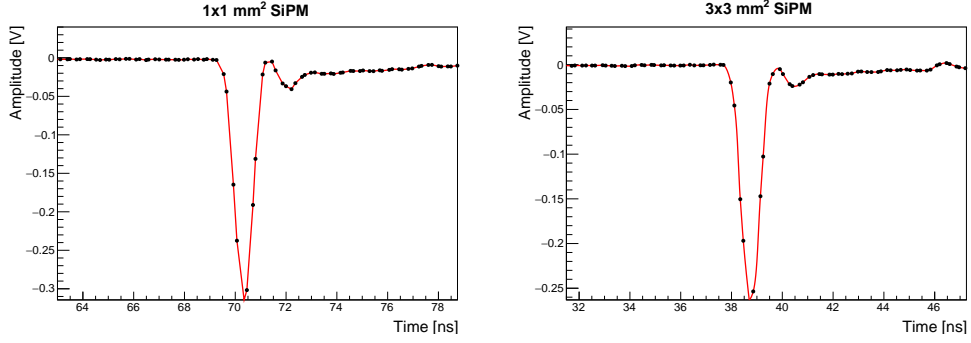


Figure 8: Digitized waveforms of the signals from the PiLas laser in the S12571-015P and S12572-25C SiPMs.

210 Using several different ND filters we controlled the intensity of the photon beam
 211 impinging upon the SiPMs under test and achieved a large dynamic range of signal
 212 sizes ranging from a single incident photon to a few hundred. In Figure 9, we show
 213 the integrated charge distribution for two example scenarios from which we can clearly
 214 distinguish different peaks corresponding to different number of photoelectrons detected
 215 by the SiPMs.

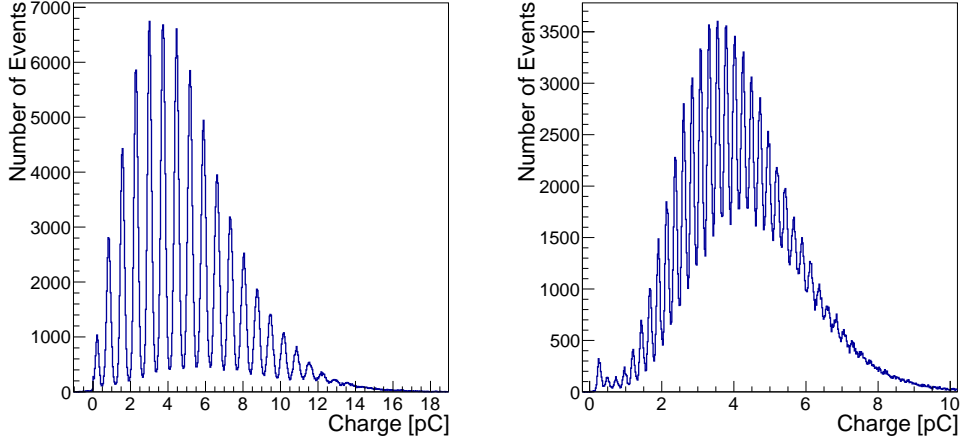


Figure 9: The distribution of integrated charge from the SiPM sensor for data taken with an ND filter of 1.8 (left), and an ND filter of 1.4 (right). A 10 db attenuator has been used for the plot on the right. The peaks corresponding to different discrete numbers of photoelectrons detected by the SiPM is clearly evident.

216 Using this setup, we measure the timestamps reconstructed from the SiPM signals

with respect to the reference MCP-PMT timestamp over an ensemble of events triggered by the external laser trigger. The sigma parameter of a gaussian fit to this distribution is taken as the time resolution measurement. As the number of photons impinging on the SiPM can be clearly distinguished based on the amplitude or charge collected, we can study the dependence of the time resolution on the number of photons. These measurements are shown in Figure 10. The amplitude for a single photoelectron signal is estimated to be 0.6 mV for the $1 \times 1 \text{ mm}^2$ S12571-015P SiPM and 0.1 mV for the $3 \times 3 \text{ mm}^2$ S12572-25C SiPM. Using these measurements, we can compare the time resolution of laser light signals on SiPMs from Figure 10 to the time resolution of electromagnetic shower signals from the WLS fiber in Figure 4 and conclude that the intrinsic timing performance of SiPM devices have very limited impact on the calorimeter time resolution. Instead, the time resolution of the calorimeter is dominated by the impact of the wavelength shifter and the corresponding increased rise time. An additional contribution to the timing resolution of the calorimeter cell may arise from longitudinal shower fluctuations. Shower depth fluctuations result in fluctuations in the time it takes for the shower to propagate into the calorimeter cell as well as for the scintillation light to propagate out of the cell through the light guides. This contribution to the time resolution is evident only if the signal is extracted at the front of the calorimeter cell because a fluctuation in the shower depth will not be compensated by a corresponding change in the optical signal transport path length. Such effects have been observed in timing studies for the CMS ECAL [16].

Finally, by removing all ND filters and increasing the laser output intensity to near maximum, we can measure the time resolution for a very large number of photons to probe for the ultimate time resolution that one could achieve with a near infinitely large signal. In Figure 11 we show the SiPM time distributions for such a scenario, and observe that the resolution is 12 ps for the $1 \times 1 \text{ mm}^2$ S12571-015P SiPM and 7 ps for the $3 \times 3 \text{ mm}^2$ S12572-25C SiPM. The measurement is also impacted by the limitation of the digitizer electronics as its time resolution is 4 ps.

5. Summary

We have presented test-beam measurements of the timing performance of a LYSO-based sampling calorimeter read out via four wavelength-shifting fibers optically coupled to silicon photomultipliers (SiPMs). Time resolutions at the level of 60 ps is achieved for beam energies above 100 GeV for individual fibers and SiPMs. Combining all four fibers yield time resolution measurements of about 42 ps. Using laser light injected directly onto SiPMs, we have demonstrated that the impact of the intrinsic time resolution of the SiPM devices is small and that the calorimeter time resolution is dominated by the impact of the wavelength shifter. Finally, we have shown that the use of quartz capillaries do not degrade the time resolution beyond the impact from a reduced signal amplitude. Therefore it is feasible that this radiation-hard solution using quartz capillaries can achieve the desired 30 ps time resolution performance if additional improvements in light collection efficiency can be achieved.

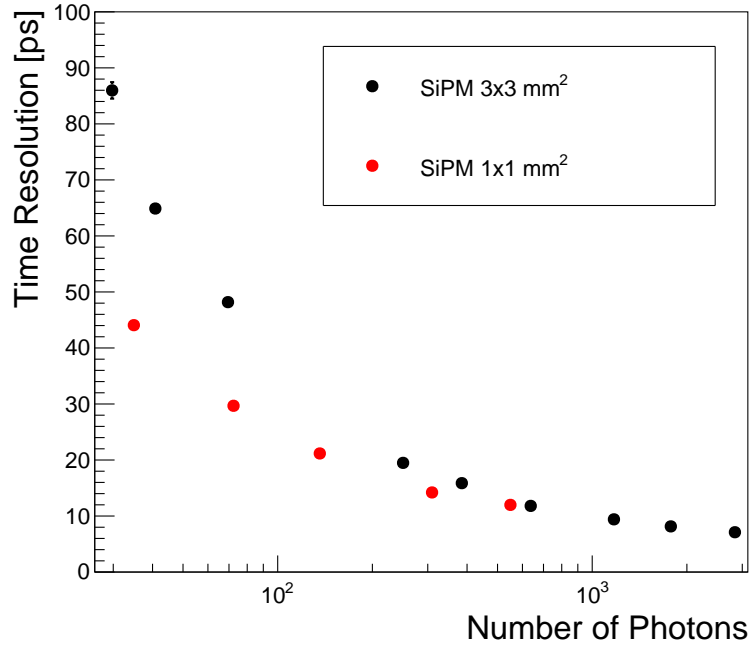


Figure 10: The time resolution is measured as a function of the number of photons impinging on the SiPMs under test. The black points show measurements using the $3 \times 3 \text{ mm}^2$ SiPM, and the red points show measurements using the $1 \times 1 \text{ mm}^2$ SiPM.

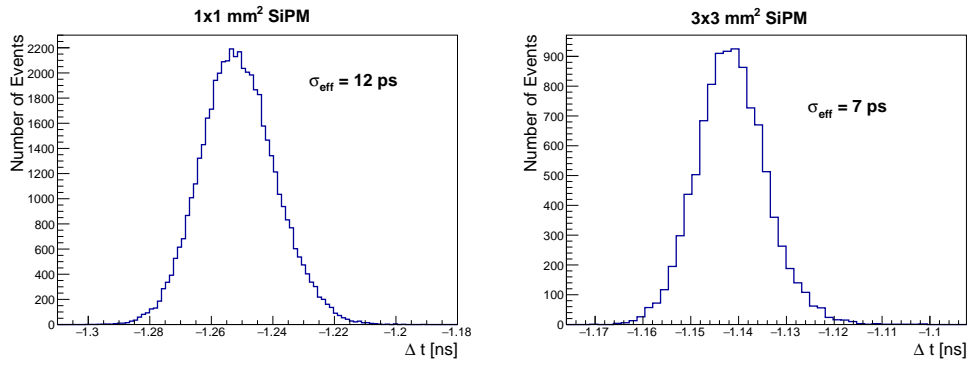


Figure 11: The SiPM time distribution and resolution measured for laser signals at high laser intensity. The resolution is characterized by σ_{eff} , which is the width obtained by integrating outwards from the peak to achieve 68% coverage.

258 6. Acknowledgements

259 Supported by funding from California Institute of Technology High Energy Physics
 260 under Contract DE-SC0011925 with the United States Department of Energy. We thank
 261 the CERN test-beam facilities personnel for excellent beam conditions during our test-
 262 beam time. We also thank Paolo Meridiani and Francesco Micheli for their kind assistance
 263 on the setup of the DAQ system at the test-beam. We greatly appreciate the collaboration
 264 with Randy Ruchti who provided us with wavelength-shifting fibers doped with DSB as
 265 well as quartz capillaries filled with liquid DSB wavelength shifter.

266 References

- 267 [1] L. Zhang, R. Mao, F. Yang, and R. Zhu, “LSO/LYSO Crystals for Calorimeters in Future HEP
 268 Experiments,” *IEEE Transactions on Nuclear Science*, vol. 61, pp. 483–488, Feb 2014.
- 269 [2] F. Yang, R. Mao, L. Zhang, and R.-Y. Zhu, “Characterization of three LYSO crystal batches,”
 270 *Nucl. Instrum. Meth.*, vol. A784, pp. 105–110, 2015.
- 271 [3] A. Bornheim, “On the Usage of Precision Timing Detectors in High Rate and High Pileup Envi-
 272 ronments,” *PoS(Vertex2016)044*, 2016.
- 273 [4] N. Neri, A. Cardini, R. Calabrese, M. Fiorini, E. Luppi, U. Marconi, and M. Petruzzo, “4D fast
 274 tracking for experiments at high luminosity LHC,” *JINST*, vol. 11, no. 11, p. C11040, 2016.
- 275 [5] C. Aberle, A. Elagin, H. J. Frisch, M. Wetstein, and L. Winslow, “Measuring Directionality in
 276 Double-Beta Decay and Neutrino Interactions with Kiloton-Scale Scintillation Detectors,” *JINST*,
 277 vol. 9, p. P06012, 2014.
- 278 [6] E. Oberla and H. J. Frisch, “The design and performance of a prototype water Cherenkov optical
 279 time-projection chamber,” *Nucl. Instrum. Meth.*, vol. A814, pp. 19–32, 2016.
- 280 [7] A. Heering *et al.*, “Effects of very high radiation on SIPMs,” *Nucl. Instrum. Meth.*, vol. A824,
 281 pp. 111–114, 2016.
- 282 [8] Y. Musienko *et al.*, “Radiation damage studies of silicon photomultipliers for the CMS HCAL phase
 283 I upgrade,” *Nucl. Instrum. Meth.*, vol. A787, pp. 319–322, 2015.
- 284 [9] S. Ritt, R. Dinapoli, and U. Hartmann, “Application of the DRS chip for fast waveform digitizing,”
 285 *NIM A 623 (2010) 486-488*.
- 286 [10] A. Ronzhin, S. Los, E. Ramberg, A. Apresyan, S. Xie, M. Spiropulu, and H. Kim, “Study of the
 287 timing performance of micro channel plate photomultiplier for use as an active layer in shower
 288 maximum detector,” *Nucl. Instrum. Meth.*, vol. 795, pp. 288–292, 2015.
- 289 [11] D. Anderson, A. Apresyan, A. Bornheim, J. Duarte, C. Pena, A. Ronzhin, M. Spiropulu, J. Trevor,
 290 and S. Xie, “On Timing Properties of LYSO-Based Calorimeters,” *Nucl. Instrum. Meth. A*, vol. 794,
 291 pp. 7–14, 2015.
- 292 [12] http://www.hamamatsu.com/resources/pdf/ssd/mppc_kapd0004e.pdf.
- 293 [13] H. Li, “Longevity of the CMS ECAL and Scintillator-Based Options for Electromagnetic Calorime-
 294 try at HL-LHC,” *IEEE Trans. Nucl. Sci.*, vol. 63, no. 2, pp. 580–585, 2016.
- 295 [14] L. Zhang, R. Mao, F. Yang, and R. Y. Zhu, “Lso/lyso crystals for calorimeters in future hep
 296 experiments,” *IEEE Trans. Nucl. Sci.*, vol. 61, pp. 483–488, Feb 2014.
- 297 [15] B. Baumbaugh *et al.*, “Studies of wavelength-shifting liquid filled quartz capillaries for use in a
 298 proposed CMS calorimeter,” in *Proceedings, 2015 IEEE Nuclear Science Symposium and Medical
 299 Imaging Conference (NSS/MIC 2015): San Diego, California, United States*, p. 7581951, 2016.
- 300 [16] Simone Pigazzini for CMS Collaboration, “Precision timing with PbWO crystals and prospects for
 301 a precision timing upgrade of the CMS electromagnetic calorimeter at HL-LHC.” CALOR 2016,
 302 2016.